Band (UWB) Networks with Uncontrolled Interference

Alaeddine El Fawal and Jean-Yves Le Boudec
School of Computer and Communication Sciences
Ecole Polytechnique Fédérale de Lausanne (EPFL)
{alaeddine.elfawal, jean-yves.leboudec}@epfl.ch

***Abstract*— We propose a novel detection method for non-coherent synchronization (signal acquisition) in multi-user UWB impulse radio (IR) networks. It is designed to solve the IUI (Inter-User Interference) that occurs in some ad-hoc networks where concurrent transmissions are allowed with heterogeneous power levels. In such scenarios, the conventional detection method, which is based on correlating the received IR signal with a Template Pulse Train (TPT), does not always perform well. The complexity of our proposal is similar to that of the conventional method. We evaluate its performance with the Line Of Sight (LOS) and the Non LOS (NLOS) office indoor channel models proposed by the IEEE P802.15.4a study group and find that the improvement is significant. We also investigate the particular case where the concurrent transmissions have the same time-hopping code, and we show that it does not result in collision, such scenarios appear in ad-hoc networks that employ common code for control or broadcast purposes.**

***Index Terms*— Ultra Wide Band (UWB), signal acquisition, Inter-User Interference, Near-Far scenario, concurrent transmissions.**

I. Introduction

WE PROPOSE a novel detection method, called PID (Power Independent Detection) method, for non-coherent synchronization in multi-access Ultra Wide Band (UWB) Impulse Radio (IR) networks. To understand what we mean by detection method, let us define the following terminology. We consider the synchronization of one receiver to one sender (also called signal acquisition). We are interested in methods based on the correlation of the IR signal with a Template Pulse Train (TPT). Such methods involve two ingredients: (1) the detection, which correlates the received signal with a TPT, we refer to this detection method as the conventional detection method, and (2) the search algorithm, which shifts the TPT. We focus on detection. Our proposal aims at solving the extreme Inter-User Interference (IUI) case (near-far problem), when there are multiple interfering transmitters, asynchronous transmissions and heterogeneous power levels. This occurs for example in the presence of multiple interfering piconets, or in purely ad-hoc networks that allow concurrent transmissions, always at full power [2], [3]. As a typical example, we can imagine headphones set employing the IR UWB technology to exchange music with some master device such as a laptop. People may use these headphones with different masters in an office environment or even in the same room. They may move or exchange places, which creates very harmful interference. Another application could be the sensor networks where the IR UWB technology is a potential candidate because of its low power consumption. We can imagine tens or even hundreds of sensors deployed in a small area communicating with each other in an ad-hoc fashion with a huge amount of interference. In such scenarios the conventional detection method faces a certain failure in the absence of power control which may entail a prohibiting overhead. Further, according to [4] the optimal is to allow sending at full power and to apply rate adaptation but not power control.

Our PID method solves the problem without any additional complexity overhead, e.g. for a digital receiver, it employs the same sampling frequency and number of operations as the conventional detection method. Unlike the conventional detection method, the PID method splits the correlation into elementary correlations, each one corresponds to one pulse in the TPT. Then, two threshold checks are performed. The first is to detect pulses whereas the second is to detect the signal based on the number of detected pulses. To evaluate the performance of the PID method, we propose a hybrid method combining analysis and simulation that is carried out according to the Line Of Sight (LOS) and the Non LOS (NLOS) office indoor channel models proposed by the IEEE P802.15.4a study group [5]. The results presented in the end show a significant improvement compared to the conventional detection method.

Furthermore, we investigate the particular case where the concurrent transmissions have the same time-hopping code; such scenarios appear in ad-hoc networks that employ common time-hopping code for control or broadcast purposes as in [2]. We show that, with high probability, this kind of transmissions does not result in collision, i.e. one signal is detected and the others are simply ignored. Further, with the conventional method, the user with the highest power is most likely the one that is detected, whereas with our method, all users within the

The work presented in this paper was supported (in part) by the National Competence Center in Research on Mobile Information and Communication Systems (NCCR-MICS), a center supported by the Swiss National Science Foundation under grant number 5005-67322.

This work has been presented in part at the ICU 2005, IEEE International Conference on UWB [1].

detactability range have the same probability of being detected.

The paper is organized as follows. In section II, we start by a discussion of the related work. In section III, we describe the system model and state the problem we will address. In section IV, we list the definitions of all notations used globally through the paper. In section V, we review the conventional detection method and explain its shortcoming. Our proposal, the PID method, is detailed in section VI. In section VII, we explain how we proceed to evaluate the PID method, and the results, including those of the asynchronous concurrent transmissions with the same code, are shown in section VIII. We conclude the paper in section IX.

II. Related Work

In [6] and [7] a frequency domain approach is adopted using subspace-techniques and least-squares methods in order to detect the arrival time of the IR signal. But only a single user transmission is considered without any IUI, unlike what we do.

In [8]–[10], synchronization methods for differential receivers are developed; In [8], [10], the proposed methods achieve frame level synchronization, whereas detecting only the presence of the signal is ensured in [9]. The authors in [11] give a sequence timing estimation which relies on the cyclostationarity that arises only when there is no Time Hopping (TH) within each sequence and requires dense multipath that fills up the frame. The four methods of [8]–[11] do not operate well in case of the near-far problem, unlike our proposal.

In this paper, we are interested in the synchronization methods that employ the conventional detection method, which give an accurate timing (pulse level synchronization) by detecting the arrival time of the IR signal. Furthermore, these synchronization methods detect the polarity of the signal. The conventional detection method has been recently adopted in a large number of references, in combination with a variety of search algorithms; some search algorithms are adequate for fine grained synchronization (e.g. serial [12]) or for coarse synchronization (e.g. "Look and Jump K" [13], Bit reversal [14]–[16], sequential block search [17] and n-scaled acquisition algorithms [18]). It suffers from the near-far problem with all these search algorithms. Our proposal, the PID method, is designed to replace it and solve the near-far problem with all the search algorithms. Further, the PID method can be generalized to the aforementioned work of [8]–[11] for the same purpose.

To our knowledge, this is the first work that identifies the problem of the conventional detection method in the presence of concurrent transmissions with heterogeneous power levels. Furthermore, the case of the asynchronous concurrent transmissions with the same code has not been discussed in the literature before.

Note that this paper is an extended version of the work presented in [1]: The main differences are that (1) this version exposes in detail the problem and involves more explanations to make the reader more comfortable, (2) it includes the analysis used to evaluate the PID method, which is not presented in [1], (3) in addition to the LOS case, it studies the case of NLOS, which is not exposed in [1] and (4) it shows the feasibility of the asynchronous concurrent transmissions with the same code.

III. Model and Assumption

An IR signal consists of trains of very short pulses to the order of a nanosecond or even a sub-nanosecond. In this paper we consider a Time Hopping (TH) physical layer proposed by Win-Scholtz [19]. TH is ensured using a pseudo-random code of length L_c. Such a physical layer can employ several modulation schemes such as BPSK (Binary Phase Shift Keying), PPM (Pulse Position Modulation), PAM (Pulse Amplitude Modulation); we do not have to specify a modulation scheme here since there is no data transmitted during the synchronization period and thus the signal we treat is not modulated. The transmitted signal of the m^{th} user is:

$$s^{(m)}(t) = \mathscr{E}^{(m)} \sum_{j} \sum_{k=1}^{L_c} p\left(t - (c_k^{(m)} - 1)T_c - (k-1)T_f - jT_s - \tau_X^{(m)}\right) \quad (1)$$

where $p(t)$ is the second derivative of the Gaussian pulse. We have chosen this pulse because we assume that the transmitter generates the Gaussian pulse, which undergoes 2 derivations at the transmitter and receiver antennas respectively. Thus, to simplify the notation we consider only the pulse received at the correlator, which is the second derivative of the Gaussian pulse, instead of using three different pulses. This simplification does not change the results of this study. $\mathscr{E}^{(m)}$ is to indicate the signal amplitude, T_c is the chip duration, $c_k^{(m)}$ is the k^{th} element of the m^{th} user code, i.e. the number of the chip that corresponds to the pulse position in the k^{th} frame of a m^{th} user sequence, $T_f = N_c \times T_c$ is the frame duration where N_c is the number of chips in one frame, T_s is the sequence duration, that is $T_s = T_f \times L_c$ and $\tau_X^{(m)}$ is the transmission start time. We assume that the pulse width and the chip duration are equal.

For our results, we consider the Saleh-Valenzuela (SV) channel model adopted in [5]. For simplicity, we express its impulse response using the well-known tapped delay line expression:

$$h(t) = \sum_{l=1}^{L} a_l \delta(t - t_l) \quad (2)$$

where $\delta(t)$ denotes the Dirac impulse, t_l the signal delay along the l^{th} path and a_l is a real propagation coefficient that includes the channel attenuation and the polarity of the signal along the l^{th} path. Then the received signal is given by:

$$r(t) = \sum_{m=1}^{M} \sum_{l=1}^{L^{(m)}} a_l^{(m)} s^{(m)}\left(t - t_l^{(m)}\right) + n(t) \quad (3)$$

where M is the number of users in the network and $n(t)$ is the White Gaussian noise.

Assume that the receiver is interested in detecting the signal sent by the first user. Then, the objective of the synchronization methods that use either the PID or the conventional detection

methods is to detect whether the first user is transmitting or not, and if he is transmitting, they find the arrival time of one sequence in the first user signal according to one of the multipath components, i.e. they find one value of $\left\{\left(\tau_X^{(1)} + jT_s + t_l^{(1)}\right),\ l = 1, \ldots, L,\ j = 0,\ 1,\ \ldots\right\}$, let τ_0 be the found value. Further it detects the sign of the corresponding a_l.

In our simulation, we consider a frame time, T_f, larger than the delay spread of the channel in order to minimize the inter-symbol interference. We assume the channel is stationary during the synchronization phase. We do not make any assumption about the separation of the channel taps, so pulses might or might not overlap after convolution with the channel impulse response. However, this overlapping happens rarely because we adopt a very short pulse of 0.2 ns.

IV. List of Global Notation

In the following we are listing the notations used globally through this article.

General Notations:

- FA: False Alarm
- IR: Impulse Radio
- IUI: Inter-User Interference
- LOS: Line Of Sight
- NLOS: Non Line Of Sight
- PID: Power Independent Detection
- UWB: Ultra Wide Band
- TPT: Template Pulse Train

Physical layer parameters:

- L_c: code length
- T_c: chip duration
- T_f: frame duration
- T_s: sequence duration
- $\mathscr{E}$: signal amplitude
- E_0/N_0: the bit energy to noise spectral density (one pulse is sent per bit)
- τ_0: detected arrival time

Different signals:

- $p(t)$: second derivative of the Gaussian pulse
- $r(t)$: received signal

Conventional detection method parameters:

- α_i: the output of the i_{th} elementary correlation
- β: sum of the elementary correlation outputs with the conventional detection method
- γ: the threshold with the conventional detection method

PID method parameters:

- α_i: the output of the i_{th} elementary correlation
- θ: the elementary threshold with the PID method
- χ: sum of the elementary threshold check outputs with the PID method
- φ: the main threshold with the PID method

Complete synchronization method parameters:

- χ_{max}: the largest χ obtained during the first phase or one iteration of the second phase of the PID synchronization method
- $\varphi^{(1)}$: the value of φ during the first phase
- $\varphi^{(2)}$: the value of φ during the second phase
- A: number of iterations in the second phase
- B: minimum number of succeeded threshold checks during the second phase so that detection is declared
- SB: the signal bin detected in the first phase of the complete synchronization method
- V: a predefined neighborhood of SB used for the search in the second phase

Probability notations:

- P_{MD}: probability of Missed Detection
- P_{FA0}: probability of False Alarm in the absence of the true sequence
- E_t: total error, $E_t = P_{MD} + P_{FA0}$
- P_1: the probability of good detection during the first phase in the presence of the true sequence
- P_2: the probability of a bad detection during the first phase in the absence of the true sequence
- P_3: the probability that one threshold check succeeds during the second phase, given that the first phase has resulted in a good detection in the presence of the true sequence
- P_4: the probability that one threshold check succeeds during the second phase, given that the first phase has resulted in a bad detection in the absence of the true sequence

V. Conventional Detection Method

A. Description

As it is explained in section I, we consider synchronization methods that involve two ingredients: the detection and the search algorithm. With the conventional detection method, the received IR signal is correlated with a TPT, which is a replica of the sequence used by the first user and which is given by:

$$s_{TPT}(t) = \sum_{k=1}^{L_c} p\left(t - (c_k^{(1)} - 1)T_c - (k-1)T_f\right) \qquad (4)$$

The idea behind the correlation is to compare the TPT with the received impulse radio signal, which may or may not have the identical pattern of pulses as the TPT. Then a threshold check is performed on the output of the correlation (β in (5)) to detect whether there is a match (an alignment) between the TPT and the received IR signal.

The role of the search algorithm is to shift the TPT with predefined time offsets so that the TPT is placed at various locations in time as compared to the received impulse radio signal until a match is obtained between them, i.e. they are aligned. The output of the cross-correlator is:

$$\beta = \int_{\sum_{i=1}^{n} \text{Offset}_i}^{\sum_{i=1}^{n} \text{Offset}_i + T_s} r(t) s_{TPT}\left(t - \sum_{i=1}^{n} \text{Offset}_i\right) \mathrm{d}t \qquad (5)$$

where n is the current shift number and Offset_i is the time offset at the i^{th} shift of the TPT. (5) is known in the literature as a coherent integration, but in this paper we refer to it as a correlation between the TPT and the received IR signal (note that we do not assume that the receiver knows the channel). The receiver gets synchronized with the transmitter at the n^{th} offset if $\sum_{i=1}^{n} \text{Offset}_i$ is equal to one value of the set $\left\{\left(\tau_X^{(1)} + jT_s + t_l^{(1)}\right),\ l = 1, \ldots, L,\ j = 0,\ 1,\ \ldots\right\}$, and thus $\tau_0 = \sum_{i=1}^{n} \text{Offset}_i$. Notice that, according to (4), (5) can

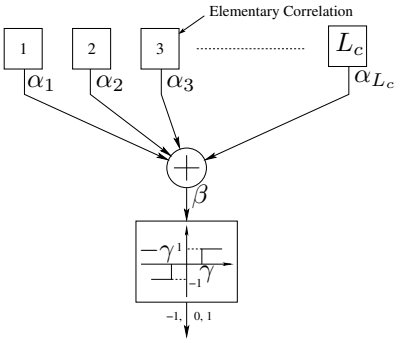

Fig. 1. The conventional detection method can be interpreted as L_c elementary cross-correlations. Block i, $i = 1, \ldots, L_c$, presents the correlation of the i^{th} pulse in the TPT with its corresponding interval.

be interpreted as L_c elementary correlations $\{(\alpha_k)\}$, $k = 1, \ldots, L_c$. α_k is the output of the elementary correlation k that corresponds to the k^{th} pulse in the TPT. We can write:

$$\beta = \sum_{k=1}^{L_c} \alpha_k \ , \tag{6}$$

where:

$$\alpha_k = \int_{(c_k^{(1)}-1)T_c+(k-1)T_f+\sum_{i=1}^{n}\text{Offset}_i}^{(c_k^{(1)}-1)T_c+(k-1)T_f+\sum_{i=1}^{n}\text{Offset}_i+T_c} p\left(t - (c_k^{(1)}-1)T_c - (k-1)T_f - \sum_{i=1}^{n}\text{Offset}_i\right) r(t)\mathrm{d}t \tag{7}$$

These L_c elementary correlations correspond to the L_c correlations of the TPT *pulses* and their corresponding intervals of the IR signal. In Fig. 1, the L_c elementary correlations are presented by the blocks indexed from 1 to L_c. β is the input of the decision block, which in turn performs a threshold check. Hence, a match between the TPT and the IR signal is declared if the absolute value of β exceeds certain threshold γ. Note that a (-1) output of the decision block means that a match is declared but the signal is inverted due to reflection, i.e. the corresponding a_l is negative (see previous section).

B. Example Showing the Problem with the Conventional Detection Method

To show the inefficiency of the conventional detection method, we present one scenario that is based on the measurement made by M. Win and R. Scholtz in [20] for an indoor environment. Consider a source (user 1) that is 10 m from the receiver. The measurement in [20] gives that the amplitude of the strongest source pulse seen by the receiver is in the order of 0.03V. Assume now that there is an interferer (user 2) that is 1m from the receiver. The measured amplitude of the interfering pulse is of 1V, 33 times higher than the source pulse. Refer by $\mathscr{E}_r^{(1)}$ ($\mathscr{E}_r^{(2)}$ respectively) to the source (interferer respectively) signal amplitude at the receiver, we have $\mathscr{E}_r^{(2)} \approx 33\mathscr{E}_r^{(1)}$. Let $\alpha_0^{(1)}$ ($\alpha_0^{(2)}$ respectively) be the output of the correlation between one source (interferer respectively) pulse and one TPT pulse when they are aligned, we can write:

$$\alpha_0^{(1)} = \mathscr{E}_r^{(1)} \int_0^{T_c} p^2(t)\mathrm{d}t \ = \ \frac{\mathscr{E}_r^{(2)}}{33} \int_0^{T_c} p^2(t)\mathrm{d}t \ \approx \frac{\alpha_0^{(2)}}{33} \tag{8}$$

$\alpha_0^{(2)}$ is 33 times larger than $\alpha_0^{(1)}$. Note that when the source signal and the TPT are perfectly aligned, neglecting the interference and noise effects, β is equal to $L_c \times \alpha_0^{(1)}$. Consequently, γ can not be larger than $L_c \times \alpha_0^{(1)}$, otherwise the source signal can not be detected. If $L_c \leq 33$, it is sufficient to have one interfering pulse aligned with one TPT pulse to get a False Alarm (FA).

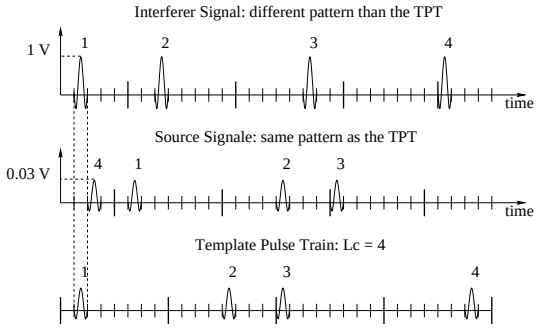

Fig. 2. A scenario showing the problem with the conventional synchronization method. The Source signal has the same pattern as the TPT but shifted in time. The interferer signal, which is 33 times stronger than the source signal, has one pulse aligned with one pulse of the TPT.

Fig. 2 illustrates this scenario with $L_c = 4$. The source signal has the same pattern as the TPT but it is shifted in time. Corresponding pulses in the TPT and the source signal carry the same number. As we notice there is one interferer pulse (pulse number 1 of the interferer signal) that is aligned with pulse number 1 of the TPT. In this case, an FA will occur since the code length L_c is very small compared to the ratio between the source and the interferer signals.

To avoid this FA, but still using the conventional detection method, L_c must be much larger than 33, which would be an extremely unaffordable overhead in term of synchronization time, since the synchronization time is proportional to the code length L_c [21]. Note that, when the number of concurrent transmissions increases, the situation becomes worse.

To summarize this example, the synchronization is either unfeasible or entails an extremely large overhead using the conventional detection method in non-power control IR networks when concurrent transmissions are allowed.

VI. Our Proposal: Power-Independent Detection Method

The idea behind the cross-correlation between the TPT and the IR signal is to detect a match between them. We need to find in the IR signal L_c pulses that have the same pattern as the TPT. But the conventional detection method does not do this. It looks at the energy captured by the correlation between the TPT and the received IR signal, which is indicated by β in Fig. 1, regardless of its distribution over the L_c elementary correlations. So, if this energy, β, is larger than the threshold, we say that the synchronization is achieved. But what happens if all the energy comes from one elementary correlation, e.g. $\beta = \alpha_1$ and $\alpha_k = 0$, $k = 2, \ldots, L_c$? This is the challenge in the scenario shown in section V-B in the case where $L_c \leq 33$. Unlike

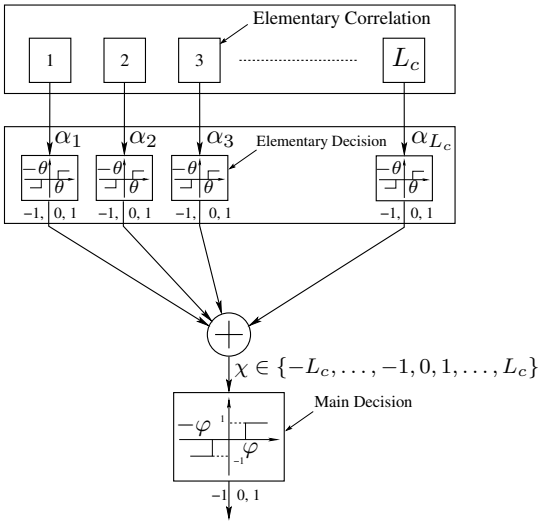

Fig. 3. PID method: each pulse is detected based on an elementary decision block. The final detection decision is based on the number of pulses detected.

the conventional detection method, the PID method solves the problem by looking at the individual energy captured by each elementary correlation separately, i.e. by looking at each α_k separately, $k = 1, \ldots, L_c$. Fig. 3 describes the architecture of our proposal; the output of each elementary correlation α_k, $k = 1, \ldots, L_c$, passes through an elementary decision block that performs an elementary threshold check. If the absolute value of α_k is larger than the elementary threshold θ, then a pulse is detected and the output of the elementary decision block k will be 1 or -1 depending on the sign of α_k (-1 means the detected pulse has negative polarity). Otherwise it will be 0. Let χ be the sum of the L_c *Elementary Decision* block outputs, we have:

$$\chi = \sum_{k=1}^{L_c} \left(\mathbf{1}_{\{\alpha_k \geq \theta\}} - \mathbf{1}_{\{\alpha_k \leq -\theta\}} \right) \in \{-L_c, \ldots, 0, \ldots, L_c\} \quad (9)$$

Thus, χ is an integer that gives the number of detected pulses, unlike β in Fig. 1 which is a real number indicating the gathered energy. If the absolute value of χ is larger than the main threshold φ, the output of the main decision block will be 1 or -1 (detected path is with negative polarity) and thus a match will be declared between the IR signal and the TPT. In the opposite case the output of the main decision block will be 0. φ should be a positive integer less than L_c, unlike γ in Fig. 1 wich can be a real number indicating the minimum of the required energy for detection.

It is intuitively clear that this new method should solve the problem described in section V-B; it is designed for an environment without power control since it is sensitive to the existence of a pulse not to its power (assuming it has enough energy to be detected). So we call our proposal "Power-Independent Detection".

VII. Performance Evaluation Method

We evaluate the performance of PID and compare it to the conventional detection method.

A. How to Evaluate the Performance

For a meaningful performance evaluation of the conventional detection and the PID methods, we imbedded them in a complete synchronization method, which consists of an identification phase, followed by a verification phase. Each phase uses the two aforementioned ingredients of detection and search algorithm iteratively. For the latter, we adopted serial search. This is because we aim to evaluate the performance of the PID method independently of the impact of optimizations that use coarse synchronization.

1) The Complete Synchronization Method: When the complete synchronization method uses PID, we call it "PID synchronization method"; when it uses conventional detection, we call it "conventional synchronization method".

Let N be the number of the search bins [1]; let "true sequence" be the sequence to be detected in the received IR signal; it has the same pattern as the TPT at the receiver.

The PID synchronization method consists of two phases. Figs. 4 and 5 illustrate the flowcharts of the first and the second phases respectively.

In the first phase, the procedure in Fig. 3 without the main decision block, i.e. block D, is repeated for the N search bins according to the serial search algorithm; we start with bin 1, then bin 2 till bin N. The largest χ, χ_{max}, is memorized, as well as its corresponding search bin. Then χ_{max} is compared to a first mean threshold, $\varphi^{(1)}$. If the absolute value of χ_{max} is strictly above $\varphi^{(1)}$, the bin that corresponds to χ_{max} is considered as a signal bin[2], SB, and we move to the second phase. Otherwise, the procedure of the first phase starts anew.

In the second phase we aim to verify the detection of the first phase. It consists of A iterations, in each one the procedure is

[1] In all conventional synchronization methods, the sequence is divided into N search bins. The bin width is equal to a small fraction of the pulse width. If σ is the bin width, we have $N = L_c \times N_c \times T_c/\sigma \, bins$. The TPT shift offset is a multiple of the bin width and it determines which bin to be searched, i.e to which bin the TPT is shifted. In another word, the bin width gives the shift resolution. After each shift, L_c elementary correlations are done, each one over the whole pulse width T_c and not the bin width (see (8)).

[2] We refer by a signal bin to the bin that corresponds to a match between the TPT and the received IR signal.

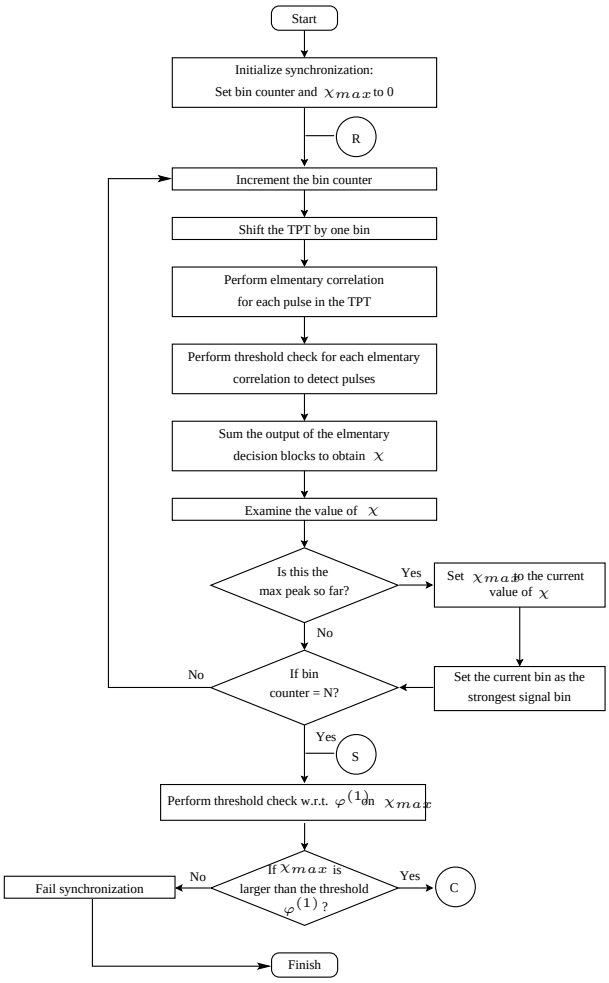

Fig. 4. The first phase of the PID synchronization method that finds the signal bin, SB, that corresponds to the highest value of χ above the first main threshold $\varphi^{(1)}$.

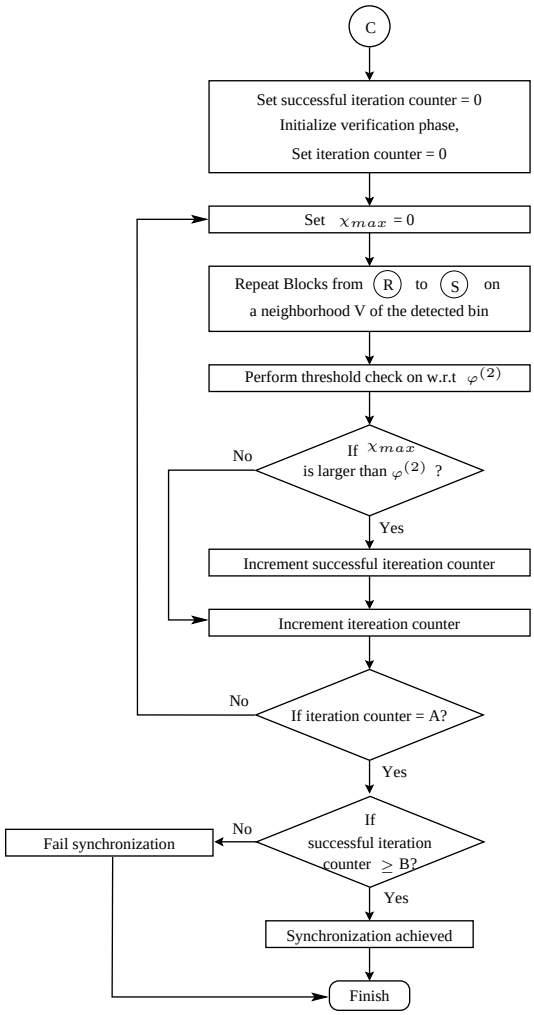

Fig. 5. The second phase of the PID synchronization method that verifies the detection declared in the first phase. It consists of A iterartions similar to the first phase but applied on a predefined neighborhood of SB and with a higher second main threshold $\varphi^{(2)}$.

the same as in the first phase but on a predefined neighborhood of SB, V, including SB, instead of the whole N bins, and with a second mean threshold, $\varphi^{(2)}$, that is larger than $\varphi^{(1)}$. If at least B threshold checks among A succeed, the detection is confirmed, otherwise the detection of the first phase is cancelled and the procedure of the first phase starts anew.

The conventional synchronization method is similar to the PID synchronization method with the difference that it does not perform a threshold check on the elementary correlation outputs.

2) Performance Metrics: We measure the performance of each procedure by the following metrics, applied to the synchronization method: (1) the probability of Missed Detection (P_{MD}) in the presence of the true sequence in the received IR signal (2) the probability of False Alarm, P_{FA0}, in the absence of the true sequence in the received IR signal and (3) the total error defined as $E_t = P_{MD} + P_{FA0}$. Note that P_{MD} includes both errors that can occur in the presence of the true sequence: the probability of false alarm and the probability of no detection.

B. Computation of Metric Using Hybrid Method: Analysis + Simulation

1) Analysis: The goal of the analysis is to express the metrics as functions of other probabilities that we obtain by simulation. The probabilities are as follows: During the first phase we have P_1, the probability of good detection when the received IR signal contains the true sequence, and P_2, the probability of a bad detection when the received IR signal does not contain the true sequence. During the second phase we define P_3 as the probability that one threshold check succeeds, given that the first phase has resulted in a good detection in the presence of the true sequence and P_4 as the probability that one threshold check succeeds, given that the first phase has resulted in a bad detection in the absence of the true sequence.

The Analysis presented in Appendix I gives:

$$P_{MD} = 1 - P_1 \sum_{i=B}^{A} \binom{A}{i} P_3^i \left(1 - P_3\right)^{(A-i)} \qquad (10)$$

$$P_{FA0} = P_2 \sum_{i=B}^{A} \binom{A}{i} P_4^i \left(1 - P_4\right)^{(A-i)} \quad (11)$$

2) Simulation: In order to compute the metrics, we ran a campaign of simulations to estimate the probabilities P_i, $i = 1, \ldots, 4$. The simulations were carried out using matlab. We tried to make the simulated scenario as realistic as possible by choosing a real multipath fading channel model and by adjusting all simulation parameters, e.g. the bit energy to noise spectral density ratio E_0/N_0 (one bit corresponds to one pulse), the physical layer parameters, the transmission power levels, the number of users.

a) Channel Model: In our simulations, we consider the indoor office environment defined by the IEEE P802.15.4a study group [5] and we studied the LOS and the NLOS cases. We adopted the LOS channel model as it is proposed in [5]. As to the NLOS, only the pathloss and small scale fading parameters are available in [5] and not the delay profile parameters. Since the available parameters are extracted from [22], we also filled the missing parameters from the same work in [22] so that the model is totally coherent and compatible.

Although the measurements made for these models were using an UWB IR signal, the models is generalized to be used by any carrier modulation system. Thus, the phase of a multipath component is considered as uniformly distributed over [0,2π] which is meaningless in an UWB IR baseband transmission. We solve this problem by relaxing this hypothesis and replacing it by the one adopted in [23], which is appropriate for IR baseband transmission. Then, the phase of a multipath component will be $0/\pi$ with an equal probability for representing pulse inversion due to the reflection from different surfaces.

For simplicity, we assume that the distribution of the small scale fading is Rayleigh instead of Nakagami since the mean value in dB of the "m" parameter of the Nakagami distribution in the adopted model is very close to zero, which corresponds to the particular case of the Rayleigh distribution.

b) Simulation Parameters: We consider that all users are sending non-modulated IR signals, an assumption that does not affect our results since the interferer signals are already random with respect to the receiver and using data modulation will add one more random variable with zero mean. We have $T_c = 0.2ns$. N_c is set, in the LOS case, to 200 chips/frame that corresponds to $40ns$, which is sufficient to minimize the inter-symbol interference due the multipath delay spread [22], [24]. In the NLOS case, N_c is set to 400 chips/frame since the multipath delay spread is larger [22], [24]. Further, the cardinality of the code is set to 100, i.e. a source can place a pulse in only the first 100 chips of a frame. The sampling frequency is 50 GHz, much larger than the Nyquist sampling frequency, to simulate an analog receiver since the impact of the sampling frequency is out of the scope of this study. The elementary threshold (θ in Fig. 3) is set to $0.5 \times \alpha_0^{(1)}$ (see 8) with $\mathscr{E}_r^{(1)}$ corresponds to the highest multipath components.

Each simulated scenario contains several transmitters, we refer to them as users, the one that is transmitting the true sequence is called the source and others are the interferers. In our simulations, we consider a rather pessimistic scenario where all interferers have at least the same transmit power as the source. The source signal power observed by the receiver is set to $-30dBm$, whereas the interferer signal powers observed by the receiver are uniformly distributed over [-30dBm, -10dBm]. Then the largest value of signal power that an interferer can have is 20 dB larger than the source signal power. Indeed, according to the pathloss model used in [5], this difference in power corresponds to a communication range of 17 m approximately in the LOS case and to 4.5 m in the NLOS case (see Appendix II) where all users are transmitting at the same power and the source is the farthest. Such a communication range is typical for an indoor environment and the adopted channel model of [5] is still valid since it is based on measurements that cover a range from 3 m to 28 m.

Since we assume a stationary channel during the synchronization phase, we consider a small neighborhood V of 2 pusles width ($V = 2T_c = 0.4ns$).

In all simulated scenarios, E_0/N_0, which is the bit energy to noise spectral density ratio, is computed with respect to the source signal power. In our simulations, we consider that one pulse corresponds to one bit, that is a transmitter sends one pulse per bit.

VIII. Performance Evaluation Results

In this section, we study the behavior of the PID synchronization method according to $\varphi^{(1)}$ and $\varphi^{(2)}$ and define an optimal working point. The behavior study of the conventional synchronization method is omitted since it is similar and can be deducted by analogy. Next, we compare the PID synchronization method with the conventional one. In the end, we evaluate the special case of concurrent transmissions with the same code.

The probabilities P_i, $i = 1, \ldots, 4$, are obtained by simulation. P_1 and P_2 are computed by averaging the results of 200 independent runs for each simulated scenario. A different independent noise realization is computed per run and, within the same run, a different channel realization is computed per user.

To compute P_3 and P_4, the stationarity of the channel during the synchronization should be taken into account. Thus, the computation of P_3 and P_4 is different and more complicated. We proceed as follows: for each run of the 200 runs above, if a detection is declared, 9 other runs are done with the same channel realization for each user but with different noise realization. Then, for a given scenario, if all the 200 runs above result in a detection declaration, we will have 9 additional runs for each run and thus 1800 runs for this scenario.

A. Performance Evaluation Results of the PID Synchronization Method

We ran simulations for E_0/N_0 values between 0 dB and 20 dB, L_c values between 8 and 30, and number of users between 5 and 20 users. In the extreme scenarios with low E_0/N_0 ($<$

$10dB$), short L_c (< 16) and large number of users (20 users) the performance was not so good due to a huge amount of interference and noise. But, starting from $E_0/N_0 = 10dB$ and $L_c = 16$, the performance is acceptable and the results seem to be similar. For lack of space, we show only one scenario in order to explain the behavior of the PID synchronization method and to show the optimal working point.

Fig. 6 (a), (b) and (c) show the metrics P_{MD}, P_{FA0} and E_t in the LOS case (see the legend for details). For Fig. 6 (a), the interpretation is as follows:

For a given $\varphi^{(1)}$, P_1 does not change with $\varphi^{(2)}$ because it is independent of the second phase. As for P_3, it is obvious that it is a decreasing function of the threshold $\varphi^{(2)}$ because, when this latter gets higher, it becomes more difficult to succeed the main threshold check in the second phase. According to (10), P_{MD} is decreasing with increasing P_3. Consequently, P_{MD} is an increasing function of $\varphi^{(2)}$.

For a given $\varphi^{(2)}$, on one hand, P_1 is a decreasing function of the threshold $\varphi^{(1)}$ because, when this latter gets higher, it becomes more difficult to succeed the main threshold check in the first phase. On the other hand, P_3 is an increasing function of $\varphi^{(1)}$. Indeed, P_3 is a conditional probability that χ_{max} in one iteration of the second phase is above $\varphi^{(2)}$ given that χ_{max} in the first phase is above $\varphi^{(1)}$. Thus the smallest the difference between $\varphi^{(1)}$ and $\varphi^{(2)}$ is, the smallest P_3 is. This difference decreases when $\varphi^{(1)}$ increases for a given $\varphi^{(2)}$. Consequently, P_3 increases with $\varphi^{(1)}$. According to (10), P_{MD} is a decreasing function of both P_1 and P_3. Therefore, given $\varphi^{(2)}$, it is not evident how P_{MD} varies according to $\varphi^{(1)}$ since P_1 and P_3 vary in opposite directions. Moreover the values of A and B influence the impact of the variation of P_3. For $\varphi^{(2)}$ = 18, P_{MD} increases with $\varphi^{(1)}$ when $\varphi^{(1)}$ goes from 12 to 17, but it decreases when $\varphi^{(1)}$ passes from 17 to 18.

Fig. 6 (b) shows the probability P_{FA0}. To understand the trends of the curves, a similar interpretation can be made as above. For instance, for a given $\varphi^{(1)}$, P_2 is independent of $\varphi^{(2)}$ and P_4 is a decreasing function of $\varphi^{(2)}$. Thus, P_{FA0} decreases with $\varphi^{(2)}$ for a fixed $\varphi^{(1)}$. In contrast, for a fixed $\varphi^{(2)}$, P_2 is decreasing with $\varphi^{(1)}$ whereas P_4 is increasing.

Fig. 6 (c) shows E_t. The optimal working point for this scenario is for ($\varphi^{(1)}$;$\varphi^{(2)}$) = (10;12) where E_t is minimized. On the left hand of the optimal working point, P_{FA0} is dominant and the curves imitate those of P_{FA0} in Fig. 6 (b). In contrast, P_{MD} becomes dominant on the right hand of the optimal working point and the curves at this side are similar to those of P_{MD} in Fig. 6 (a).

In the NLOS case, the curves have similar trends and we omitted them.

In conclusion, using the PID synchronization method, an optimal working point can be obtained by minimizing E_t. For this specific example, the optimal working point is $\varphi^{(1)} = 10$, $\varphi^{(2)} = 12$.

B. Comparison between the PID and the Conventional Synchronization Methods

1) LOS Case: Now, we are comparing the PID synchronization method with the conventional one in the LOS case. The NLOS case is left for the next subsection. The results that we show correspond to the optimal working point defined in VIII-A.

Fig. 7 (a) shows P_{MD} according to E_0/N_0 for both synchronization methods. Corresponding values of E_t are shown in Fig. 7 (b). Recall that E_t is upper bounded by 2 (see VII-A.2). The simulated scenario corresponds to 10 users, $L_c = 20$ and $N_c = 200$ chips/frames. As for the parameters A and B, they concern the verification phase, which aims at eliminating any false alarm due to random interference or noise. Thus, B can be seen in somehow a threshold. If the number of iterations that result in a detection exceeds B, we consider that this is due to a good detection and not to a random effect. Hence, to ensure good performance, A and B should be well tuned. We tried several values for them and we had good performance for $A = 10$ and $B = 7$. We keep these values for all the following results. As we can notice, The PID synchronization method P_{MD} is decreasing with increasing E_0/N_0 and it is very small when E_0/N_0 becomes larger than 10 dB. In contrast, with the conventional synchronization method, P_{MD} is very high and it is close to 1 even when $E_0/N_0 = 20\,dB$. E_t in Fig. 7 (b) is a decreasing function of E_0/N_0, it reaches 10^{-8} for $E_0/N_0 = 15\,dB$ with the PID synchronization method, whereas it is very close to 2 with the conventional one.

2) NLOS Case: It is obvious that the NLOS case is more challenging since it has larger delay spread and its cluster and ray arrival rates are much higher [22]. Thus, to have an acceptable performance we reduced the number of users to 5 instead of 10 with the LOS case. Also, we used a larger $N_c = 400$ chips/frame in order to compensate the larger delay spread. Fig. 8 (a) and (b) show comparison results for P_{MD} and E_t respectively. The performance is not as good as in the LOS case but our method still performs much better than the conventional one. With the PID synchronization method, E_t is around 10^{-2} whereas it is very close to 2 with the conventional one.

To summarize this section, we have shown that, with the PID synchronization method, the synchronization is achieved in the presence of the IUI with a minimal total error. In contrast, the total error is very close to 2 with the conventional synchronization method, which means a certain failure.

C. Concurrent Transmissions with the Same Code

It is often thought that concurrent transmissions with the same code result always in collision. This is not true. Let us consider first asynchronous concurrent transmissions. In this case, the different transmitted signals[3] with the same code have different arrival times at a given receiver. Since the pulse width is very short and the transmissions are asynchronized, not all

[3]Recall that a transmitted signal is that expressed in (1)

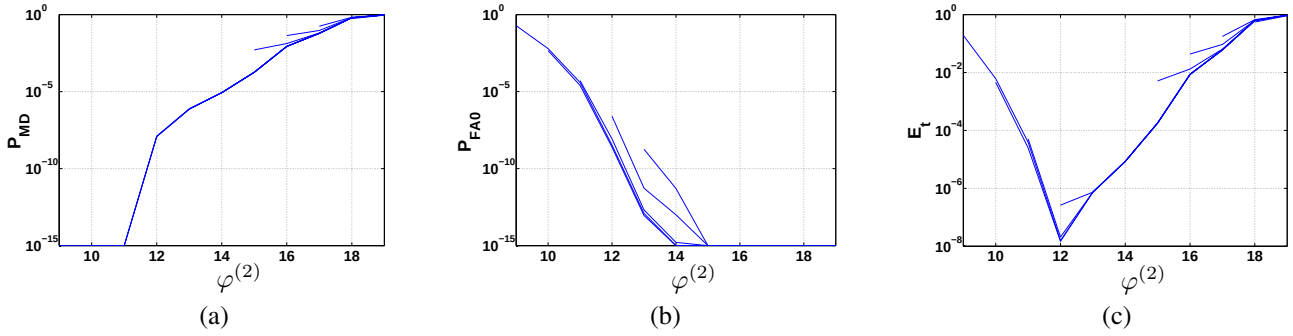

Fig. 6. Performance of PID in the LOS case for various values of the two main thresholds $\varphi^{(1)}$ and $\varphi^{(2)}$ defined in Section VII-A.1; $\varphi^{(2)}$ is on the x-axis. Each figure shows several curves that correspond to several values of $\varphi^{(1)}$. The values of $\varphi^{(1)}$ for a given curve is the x-value of its leftmost point. To understand these figures, consider the curve which leftmost point has a x-value equal to 15 in (a). It corresponds to $\varphi^{(1)}$ = 15. Since $\varphi^{(2)}$ is always larger than $\varphi^{(1)}$, this curve can not have points with x-values less than 15, which explains the different x-values of the leftmost point of these curves. The y-axis shows: (a) P_{MD} (the probability of Missed Detection), (b) P_{FA0} (the probability of False Alarm) and (c) $E_t = P_{MD} + P_{FA0}$ (the total error). E_0/N_0 = 15 dB, L_c = 20, 10 users, A = 10 and B = 7. In (a), the curves that correspond to $\varphi^{(1)}$ ranging from 9 to 14 coincide. Thus, we see only one curve instead of five. Note that we set to 10^{-15} all values that are below 10^{-15} because Matlab was not able to plot them.

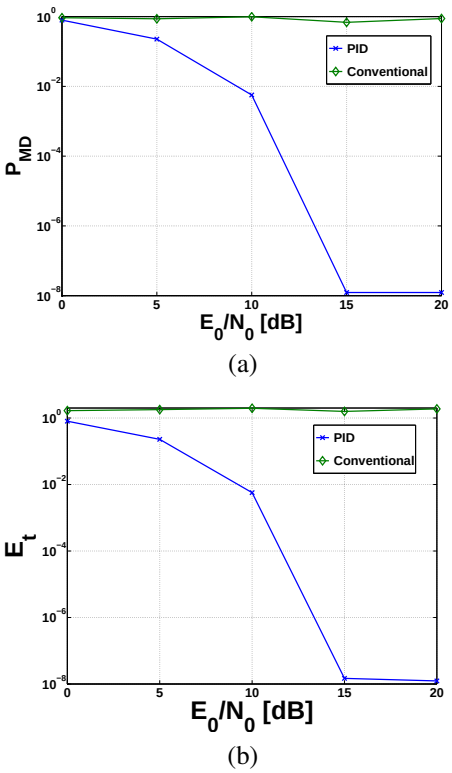

Fig. 7. A comparison between the PID and the conventional synchronization methods at the optimal working points in the LOS case. (a) P_{MD} (the probability of misdetection) and (b) $E_t = P_{MD} + P_{FA0}$ (the total error). N_c = 200 chips/frame, L_c = 20, 10 users, A = 10 and B = 7.

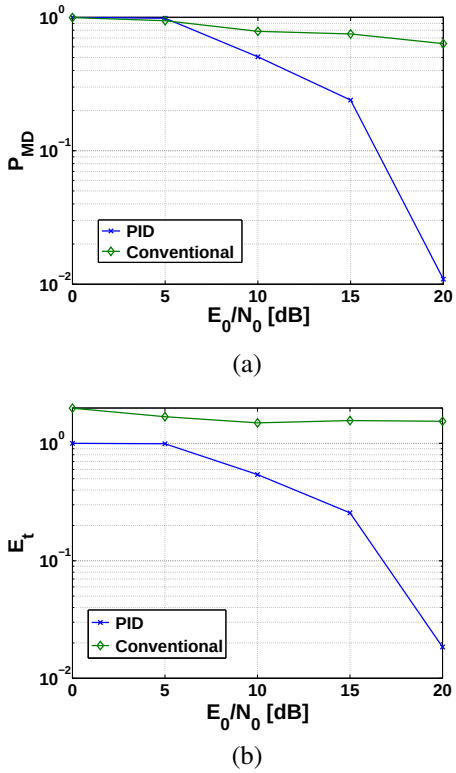

Fig. 8. A comparison between the PID and the conventional synchronization methods at the optimal working points in the NLOS case. (a) P_{MD} (the probability of Missed Detection) and (b) $E_t = P_{MD} + P_{FA0}$ (the total error). N_c = 400 chips/frame, L_c = 20, 5 users, A = 10 and B = 7.

the multipath components of the transmitted signals overlap at the receiver. Thus, the receiver can solve, with high probability, at least one multipath component that arbitrarily belongs to one of the transmitted signals. We assume that we are not in a very dense multipath environment where even transmitting with different codes results in collision. Now let us look at the extreme case where the different transmissions are synchronized and all the transmitted signals have almost the same arrival time, i.e. the first multipath components of all the transmitted signals overlap at the receiver, which happens with a negligible probability. Since each transmitted signal has a different channel impulse response, not all multipath components of the transmitted signals overlap. Therefore, the receiver can, with high probability, solve one multipath component belonging to an arbitrary transmitted signal. In the following, we show results for the asynchronous case because the other case happens very rarely and its results can be deducted from what we show here. In the simulated scenarios, E_0/N_0, L_c, $\varphi^{(1)}$ and $\varphi^{(2)}$

correspond to the optimal working point of Fig. 6. All the transmitted signals in a given run have the same code but with different arrival times and different powers chosen randomly in [-30 , -10] dBm. E_0/N_0 is computed according to a -30 dBm power signal. We did two evaluations using two different methods. The first is what we used before. The second is similar to the first but it takes into account the collisions. In the following, only P_{MD} is shown. P_{FA0} cannot be computed because the true sequence is always present in the received signal, which is the superposition of all the transmitted signals and it is expressed in (3).

1) First Evaluation: When we applied the evaluation method used before (Section VII) for a number of user up to 10 in the LOS case and to 5 in the NLOS case, P_{MD} was exactly equal to zero with the PID and the conventional complete methods. This is not surprising because all the users transmit the true sequence. Furthermore, the transmission power levels are now higher than the extreme case of Fig. 7 and Fig. 8, which even give too small $P_{MD}s$. This result does not take into account the collisions as it is explained next section.

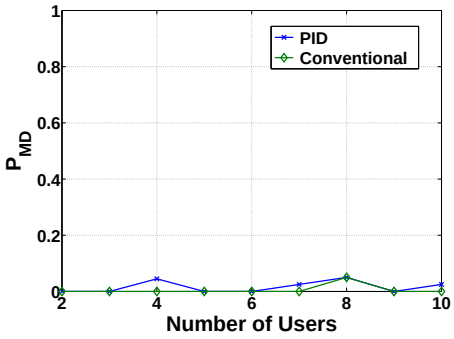

(a)

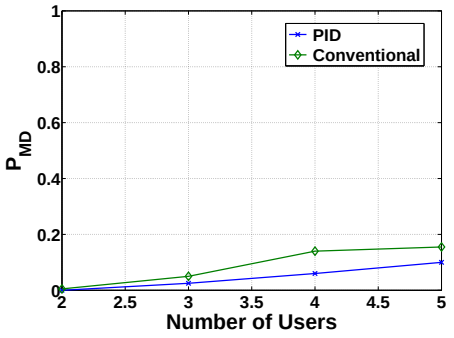

(b)

Fig. 9. P_{MD} in the case of concurrent transmissions with the same code in both cases the LOS (a) with N_c = 200 chips/frame and the NLOS (b) with N_c = 400 chips/frame. $E_0/N_0 = 15dB$, L_c = 20, A = 10 and B = 7.

2) Second Evaluation: When all the transmitted signals have the same code, the collisions become more harmful than when only one transmitted signal carries the true sequence. Indeed, since all the transmitted signals carry the same code, different multipath components of different transmitted signals may overlap in all their pulses, which do not occur in the case of different codes. Therefore, we changed p_1 to be the probability of (1) a good detection during the first phase when the received signal contains the true sequence and (2) the detected signal does not collide with another. That is when we detect some signal and we find that it overlaps with another, we consider that this is an FA and the detection is canceled.

Fig. 9 (a) and (b) show P_{MD} according to the number of users in the LOS and the NLOS cases respectively. Due to the collisions, P_{MD} is now around 10^{-1} (instead of 0 in the first evaluation). Thus, a good detection without collision is obtained with a probability of 90%. It is clear that our method performs better than the conventional one in the NLOS case, which is more challenging. This can be explained by its immunity to the constructive interference. Indeed, when two multipath components belonging to different signals have almost the same timing and thus overlap almost completely, if they have the same polarity, the resultant signal has higher amplitude which is the sum of the two multipath component amplitudes. Consequently, the probability of detecting the resultant signal, which results in a collision, increases with the conventional method since it has higher power. With our method, this probability does not change since it is power independent. We observed in our simulations that, with the PID synchronization method, all transmitted signals have the same chance to be detected independently of their power levels, which is another consequence of power independence. Also, we observed that the conventional synchronization method detects always the transmitted signal of the highest power level.

To summarize this section, concurrent transmissions with the same code do not result always in collision. Thus, the channel employing a common code, such as in [2], cannot be modeled as an Aloha channel. This modeling considers that concurrent transmissions result always in collision and, thus, it does not hold anymore.

IX. Conclusions

Our paper addresses non-coherent synchronization (signal acquisition) in the presence of asynchronous concurrent transmissions with heterogeneous power levels. This occurs, for example, in the presence of multiple interfering piconets, or in purely ad-hoc networks. This is the first work that identifies the problem that arises using the conventional detection method, which correlates the received UWB Impulse Radio (IR) signal with a Template Pulse Train (TPT) and performs a threshold check on the output of the correlation; we show that the synchronization is either unfeasible or entails an extremely large overhead due to the Inter-User Interference (IUI) in these scenarios. In order to solve the extreme IUI case (near-far problem), we propose a new detection method, which we call Power Independent Detection (PID) method; it splits the correlation into elementary correlations. Each one corresponds to one pulse in the TPT. Then, two threshold checks are performed. The first is to detect pulses whereas the second is to detect the signal based on the number of detected pulses. Our PID method solves the problem without any additional complexity overhead, e.g. for a digital receiver, it employs the same sampling frequency and number of operations as the conventional detection method.

We evaluated the performance of the PID detection method

based on analysis and simulations. The simulations were carried out according to the Line Of Site (LOS) and the Non LOS (NLOS) indoor office channel models proposed by the IEEE P802.15.4a study group [5]. The adopted metrics are (1) the probability of Missed Detection (P_{MD}) when the received IR signal contains the synchronization sequence to be detected (2) the probability of false alarm (P_{FA0}) when the received IR signal does not contain the synchronization sequence to be detected and (3) the total error defined as $E_t = P_{MD} + P_{FA0}$. The results presented in this paper show a significant improvement compared to the conventional detection method. Moreover, we define an optimal working point that corresponds to the least total error E_t. Some of the results are that, for $E_0/N_0 = 15dB$ and in the presence of 10 users transmitting simultaneously in the LOS case, $E_t = 10^{-8}$ with the PID method at the optimal working point whereas E_t is very close to 2 with the conventional detection method.

We also investigate the particular case where all concurrent transmissions have the same code: this is the case of broadcast or control channel in ad hoc networks and it may occur even in the presence of multiple interfering piconets. Our results show that, with high probability, no collision occurs and we are still able to detect one of the transmitted signals. Thus, the Aloha model does not hold anymore for this kind of channels. Further, with the conventional method, the user with the highest power is most likely the one that is detected, whereas with our method, all users within the detactability range have the same probability of being detected. Moreover, we show that the immunity of the PID synchronization method to the constructive interference makes its performance better than the conventional one in the presence of collision.

An extension of this work is to investigate how to determine the thresholds θ, $\varphi^{(1)}$ and $\varphi^{(2)}$ for these environments of concurrent transmissions with heterogeneous power levels.

Appendix I
Analysis

Our analysis treats 3 random variables, X, Y and Z, as it is indicated in Fig. 10. Block 1 represents the first phase in our synchronization method and block 2 illustrates the second phase. X is the input of block 1. Y forms the output of block 1 and the input of block 2. Z is the output of block 2. The values that X, Y and Z can take are as follows:

$$X = \begin{cases} 1 & \text{The IR signal contains the true sequence} \\ 0 & \text{Else} \end{cases}$$

$$Y = \begin{cases} 1 & \text{Good detection and X = 1} \\ 2 & \text{Bad detection either X = 0 or X = 1} \\ 3 & \text{No detection and X = 0} \\ 4 & \text{No detection and X = 1} \end{cases}$$

$$Z = \begin{cases} 1 & \text{Good detection: Y = 1 and the detection is confirmed by the second phase.} \\ 2 & \text{False Alarm: Y = 2 and the detection is confirmed by the second phase.} \\ 3 & \text{Y = 1 but the detection is canceled by the second phase.} \\ 4 & \text{Y = 2 but the detection is canceled by the second phase.} \end{cases}$$

Let P_{GD} be the probability of Good Detection, we have by definition:

$$P_{GD} = P(Z = 1|X = 1) \quad (12)$$
$$P_{MD} = 1 - P_{GD} \quad (13)$$
$$P_{FA0} = P(Z = 2|X = 0) \quad (14)$$

Introducing the variable Y in (12) we can write:

$$\begin{aligned} &P(Z = 1|X = 1) = \\ &\quad P(Z = 1|Y = 1, X = 1)P(Y = 1|X = 1) + \\ &\quad P(Z = 1|Y \neq 1, X = 1)P(Y \neq 1|X = 1) \\ &= P(Z = 1|Y = 1, X = 1)P(Y = 1|X = 1) \end{aligned} \quad (15)$$

Similarly we have for (14):

$$\begin{aligned} &P(Z = 2|X = 0) = \\ &\quad P(Z = 2|Y = 2, X = 0)P(Y = 2|X = 0) \end{aligned} \quad (16)$$

Let us express the terms on the right hand in (15) and (16) in term of P_i, $i = 1, \ldots, 4$; By definition we have:

$$P(Y = 1|X = 1) = P_1 \quad (17)$$

$$P(Y = 2|X = 0) = P_2 \quad (18)$$

$$P(Z = 1|Y = 1, X = 1) = \sum_{i=B}^{A} \binom{A}{i} P_3^i (1 - P_3)^{(A-i)} \quad (19)$$

$$P(Z = 2|Y = 2, X = 0) = \sum_{i=B}^{A} \binom{A}{i} P_4^i (1 - P_4)^{(A-i)} \quad (20)$$

Plugging (17)-(20) in (15) and (16) we obtain (10) and (11).

Appendix II
Communication Range

The mean channel pathloss excluding antenna effects is defined as [5], [25]

$$PL(d) = \frac{P_{TX}}{E\{P_{RX}(d)\}} \quad (21)$$

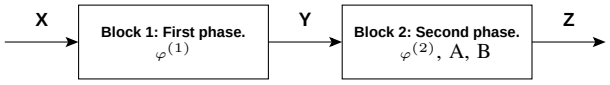

Fig. 10. The synchronization method is modeled as 2 blocks with 3 random variables. Blocks 1 and 2 represent the first and the second phases, respectively. X (input of block 1) indicates the presence of the true sequence in the received IR signal. Y (output of block 1 and input of block 2)indicates whether a detection is declared or not and, if a detection is declared, whether it is a good detection or an FA. Z (output of block 2) gives the result of the verification of the second phase.

where P_{TX} and P_{RX} are transmit and receive power, respectively, d is the distance between the transmitter and the receiver, and the expectation is taken over an area that is large enough to allow averaging out of the shadowing as well as the small-scale fading. Due to the frequency dependence of propagation effects in a UWB channel, the wideband pathloss is a function of frequency as well as distance. The pathloss as a function of distance and frequency can be written as a product of the terms

$$PL(f,d) = PL(f)PL(d). \tag{22}$$

The distance dependence of the pathloss in dB is described by

$$PL(d) = PL_0 + 10nlog_{10}\left(\frac{d}{d_0}\right) \tag{23}$$

where the reference distance d_0 is set to 1 m, and PL_0 is the pathloss at the reference distance. n is the pathloss exponent that is equal to 1.63 in the LOS case and 3.07 in the NLOS case. Then a difference of 20 dB in the pathloss between the source and an interferer that is one meter far from the receiver can be written as:

$$\begin{aligned} 20 \quad = \quad & \left(PL_0 + 10nlog_{10}\left(\frac{d_s}{d_0}\right)\right)_s - \\ & \left(PL_0 + 10nlog_{10}\left(\frac{d_i}{d_0}\right)\right)_i \end{aligned} \tag{24}$$

the indexes s and i are to indicate the source and the interferer respectively. Resolving (24) we get with the LOS case:

$$d_s = 16.86\,m \tag{25}$$

and with the NLOS case:

$$d_s = 4.48\,m \tag{26}$$

REFERENCES

[1] A. E. Fawal and J.-Y. L. Boudec, "A power independent detection method for ultrawide band (uwb) impulse radio networks," in *Proceedings of IEEE International Conference on Ultra-Wideband (ICU 2005)*, Zurich, Switzerland, Sept. 2005.

[2] M.-G. D. Benedetto, L. D. Nardis, M. Junk, and G. Giancola, "(UWB)$\hat{2}$: Uncoordinated, wireless, baseborn, medium access control for uwb communication networks," *Mobile Networks and Applications special issue on WLAN Optimization at the MAC and Network Levels*, 2005.

[3] R. Merz, J. Widmer, J. Y. L. Boudec, and B. Radunovic, "A joint phy/mac architecture for low-radiated power th-uwb wireless ad-hoc networks," *Wireless Communications and Mobile Computing Journal, Special Issue on Ultrawideband (UWB) Communications*, Aug. 2005.

[4] B. Radunovic and J. Y. L. Boudec, "Optimal power control, scheduling and routing in uwb networks," *IEEE Journal on Selected Areas in Communications*, vol. 22, no. 7, 2004.

[5] "802.15.4a channel model subgroup final report," IEEE P802.15-04-0535-00-004a, Sept. 2004. [Online]. Available: http://www.ieee802.org/15/pub/TG4a.html

[6] I. Maravic, J. Kusuma, and M. Vetterli, "Low-sampling rate uwb channel characterization and synchronization," *Journal of Communications and Networks, special issue on ultra-wideband systems*, vol. 5, no. 4, Dec. 2003.

[7] C. Carbonelli, U. Mengali, and U. Mitra., "Synchronization and channel estimation for uwb signal," in *Proc. IEEE Global Telecommunications Conf. GLOBECOM'03*, vol. 2, Dec.1-5 1997, pp. 764–768.

[8] N. He and C. Tepedelenlioglu, "Adaptive synchronization for non-coherent uwb receivers," in *Proc. IEEE Int. Conf. on Acoustics, Speech and Signal Processing ICASSP 2004*, vol. 4, Montreal, Quebec, Canada, May 2004, pp. iv–517 – iv–520.

[9] M. Pausini and G. Janssen, "Analysis and comparison of autocorrelation receivers for ir-uwb signals based on differential detection," in *Proc. IEEE Int. Conf. on Acoustics, Speech and Signal Processing ICASSP 2004*, Montréal, Canada, May 2004, pp. IV513 – IV516.

[10] L. Yang and G. B. Giannakis, "Blind uwb timing with a dirty template," in *Proc. IEEE Int. Conf. on Acoustics, Speech and Signal Processing ICASSP 2004*, vol. 4, Montréal, Quebec, Canada, May17-21 2004, pp. 509–512.

[11] Z. Tian, L. Yang, and G. B. Giannakis, "Symbol timing estimation in ultra-wideband communications," in *Proc. of 36th Asilomar Conf. on Signals, Systems, and Computers*, Pacific Grove, CA, Nov.3-6 2002, pp. 1924–1928.

[12] A. Polydoros and C. Weber, "A unified approach to serial search spread-spectrum code acquisition–part i: General theory," *IEEE Trans. Commun.*, vol. 32, no. 5, May 1984.

[13] W. Suwansantisuk and M. Z. Win, "Optimal search procedures for spread spectrum signal acquisition," in *Proc. IEEE Conf. on Inform. Sci. and Sys.*, Baltimore, MD, Mar. 2005.

[14] J. L. Richards *et al.*, "System for fast lock and acquisition of ultra-wideband signals," U.S. Patent 6 556 621, Apr. 29, 2003.

[15] E. A. Homier and R. A. Scholtz, "Hybrid fixed-dwell-time search techniques for rapid acquisition of ultra-wideband signals," in *Proc. International Workshop on Ultra-Wideband Systems*, Oulu, Finland, June2-5 2003.

[16] ——, "Rapid acquisition of ultra-wideband signals in the dense multipath channel," in *Proc. IEEE Conference on Ultra Wideband Systems and Technologies*, 2002.

[17] S. Gezici, E. Fishler, H. Kobayashi, H. V. Poor, , and A. F. Molisch, "A rapid acquisition technique for impulse radio," MITSUBISHI ELECTRIC RESEARCH LABORATORY, Tech. Rep. TR-2003-46, Aug. 2003.

[18] L. Reggiani and G. M. Maggio, "A reduced-complexity acquisition algorithm for uwb impulse radio," in *Proc. UWBST 2003*, Reston, VA, Nov. 2003.

[19] M. Z. Win and R. A. Scholtz, "Ultra-wide bandwidth time-hopping spread-spectrum impulse radio for wireless multiple-access communications," *IEEE Trans. Commun.*, vol. 48, no. 4, Apr. 2000.

[20] M. Z. Win, R. A. Scholtz, and M. A. Barnes, "Ultra-wide bandwidth signal propagation for indoor wireless communications," in *Proc. IEEE Int. Conf. Communications*, vol. 1, Montréal, Canada, June 1997, pp. 56–60.

[21] A. E. Fawal and J. Y. L. Boudec, "Fast synchronization in uwb self-organized networks and in the absence of power control," Doctoral School Project, EPFL, July 2004.

[22] B. Kannan *et al.*, "Uwb channel caracterization in indoor office environments," IEEE P802.15-15-04-0439-00-004a, Aug. 2004. [Online]. Available: http://www.ieee802.org/15/pub/TG4a.html

[23] "Channel modeling sub-committee report final," IEEE P802.15-02/490r1-SG3a, Feb. 2003.

[24] J. Foerster and Q. Li, "Uwb channel modeling contribultion from intel," Call for Contributions on Ultra-wideband Channel Models (IEEE P802/208r1-SG3a), Intel, June24 2002.

[25] S. S. Ghassemzadeh, R. Jana, C. Rice, W. Turin, and V. Tarokh, "Measurement and modeling of an ultra-wide bandwidth indoor channel," *IEEE Trans. Commun.*, vol. 52, no. 10, Oct. 2004.

Alaeddine El Fawal was born in Tripoli, Lebanon, in 1977. He received the Telecommunication and Computer engineering degree in 2001 and the master degree in Networking in 2002, both from the Lebanese University. He carried out his engineering and master thesis respectively at LCST (Laboratoire des Composants et des Systmes de Tlcommunications), INSA Rennes France, and the Plante team, INRIA Sophia Antipolis - France respectively.

He is currently working toward the Ph.D. degree with Prof. Jean-Yves Le Boudec at the School of Computer and Communication Sciences, EPFL - Switzerland. His main research interests include Ultra-Wide-Band communications, autonomic opportunistic communication, fully self-organized wireless networks and Cheating and security in wireless LANs.

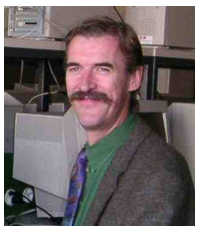

Jean-Yves Le Boudec is full professor at EPFL, fellow of the IEEE and director of the Institute of Communication Systems. He graduated from Ecole Normale Superieure de Saint-Cloud, Paris, where he obtained the Agregation in Mathematics in 1980 (rank 4) and received his doctorate in 1984 from the University of Rennes, France. From 1984 to 1987 he was with INSA/IRISA, Rennes. In 1987 he joined Bell Northern Research, Ottawa, Canada, as a member of scientific staff in the Network and Product Traffic Design Department. In 1988, he joined the IBM Zurich Research Laboratory where he was manager of the Customer Premises Network Department. In 1994 he joined EPFL as associate professor.

His interests are in the performance and architecture of communication systems. In 1984, he developed analytical models of multiprocessor, multiple bus computers. In 1990 he invented the concept called "MAC emulation" which later became the ATM forum LAN emulation project, and developed the first ATM control point based on OSPF. He also launched public domain software for the interworking of ATM and TCP/IP under Linux. He proposed in 1998 the first solution to the failure propagation that arises from common infrastructures in the Internet. He contributed to network calculus, a recent set of developments that forms a foundation to many traffic control concepts in the internet, and co-authored a book on this topic. He earned the Infocom 2005 Best Paper award with Milan Vojnovic of Microsoft Research for elucidating the perfect simulation and stationarity of mobility models.

He was on the program committee of many conferences, including Sigcomm, Sigmetrics and Infocom, was managing editor of the journal Performance Evaluation from 1990 to 1994, and is on the editorial board of ACM/IEEE Transactions on Networking.